



Exploring novel approaches for fertility and subfertility prediction in dromedary male camels (*Camelus dromedarius*)

L.O. Méar^{a,b}, G. Gnemmi^{c,d}, A. Echegaray^e, J.A. Skidmore^f, C. Malo^{g,*}

^a Laboratory of Conservation Reproductive Biology and Regenerative Medicine, Graduate Institute of Veterinary Medicine, National Taiwan University, No.1, Section4, Roosevelt Rd., Taipei 10617, Taiwan

^b Department of Reproduction Biology, Leibniz Institute for Zoo & Wildlife Research, Alfred-Kowalke Rd., No. 17, Berlin 10315, Germany

^c Bovinevet Internacional SL, Mecánica Rd., No. 9, Huesca 22006, Spain

^d Universidad Católica de Valencia (Catholic University of Valencia), Guillem de Castro Rd., No. 94, Valencia 46001, Spain

^e Humeco, Mecánica Rd., No. 11, Huesca 22006, Spain

^f Camel Reproduction Centre, PO Box 79914, Dubai, United Arab Emirates

^g Universidad de Zaragoza (Zaragoza University), Pedro Cerbuna Rd., No. 12, Zaragoza 50009, Spain

ARTICLE INFO

Keywords:

Dromedary camel
Fertility
Digital ultrasound image analysis
Prostate
Bulbourethral
Testosterone

ABSTRACT

Dromedary bulls exhibit particularly suboptimal semen quality. In this species, standard breeding soundness evaluation (BSE) often cannot catch the subtle difference between fertile and subfertile males. Therefore, the aim was to explore novel diagnostic tools to predict fertility and recognize subfertility in dromedary bulls. We explored the relationship between semen quality, fertility, echotexture parameters, accessory glands volume and total testosterone. Two sets of experiments were performed: *in vitro* (semen group) and *in vivo* (natural mating group). Each group was assessed by standard BSE: clinical examination, testis volume, ultrasound analysis of testicular parenchyma (TP) and epididymis. For the first time, images of epididymal head were obtained. Testis volume was not correlated to any parameters studied. Ultrasound TP showed especially low sensitivity (20 % *in vitro* and 14 % *in vivo*). The standard BSE was found unsuccessful in assessing subfertility. Therefore, animals were then submitted to advanced BSE: digital image analysis of TP, assessment of accessory glands (prostate (P) and bulbourethral (BB) glands) and serum total testosterone concentration. Upon analysis, significant correlations were found among some echotexture parameters (white pixels, mean grey levels, area and density of hypoechogenic areas) and percentage of viability, head defects, mitochondria potential and fertility. Only white pixels showed strong sensitivity (86 %) and specificity (100 %). BB volume correlated with ejaculate volume. Total testosterone concentration did not correlate with any parameters studied. In conclusion, advanced BSE (digital ultrasound image analysis and accessory glands volume) proved to be a useful tool for predicting semen quality and detecting subfertility in dromedary camels.

1. Introduction

The significance of dromedary camels in both milk production and racing has experienced a notable surge in recent decades, amplifying the demand for good breeders. This imperative extends beyond merely augmenting lineage, but also to better their productive parameters (Faye and Bonnet, 2012). Unfortunately, dromedary males exhibit suboptimal semen quality which highlights the importance of their reproductive management (Al-Qarawi, 2005; Rated, 2006; Faye and Bonnet, 2012; Waheed, 2014). The ability to evaluate their reproductive capacity and diagnose subfertility will enable the selection of the superior males,

thereby enhancing the outcomes of both natural and assisted breeding (Billah and Skidmore, 1992; Garde López-Brea, 1992).

Commonly, reproductive potential assessment involves conducting breeding soundness evaluation (BSE): clinical examination, testis volume and ultrasound analysis of testicular parenchyma (Rated, 2006; El-Bahrawy et al., 2015). Additionally, semen analysis is a great tool to predict fertility (Guzick et al., 2001). However, the feasibility of semen evaluation is often hindered by the challenges associated with the sample collection: training the males, sedation/anaesthesia, staff security, time-consuming, female welfare (Skidmore et al., 2018). Hence, less invasive techniques are needed to assess the reproductive capacity

* Corresponding author.

E-mail address: claramalo@unizar.es (C. Malo).

<https://doi.org/10.1016/j.smallrumres.2024.107371>

Received 30 January 2024; Received in revised form 18 September 2024; Accepted 19 September 2024

Available online 21 September 2024

0921-4488/© 2024 Published by Elsevier B.V.

and diagnose subfertility.

Ultrasonography is a non-invasive technique that has been employed in the examination of the male reproductive tract. It allows the assessment of testicular parenchyma echogenicity which provides realistic information regarding testicular histomorphology and blood flow (Giffin et al., 2009; Camela et al., 2019). Ultrasonography can also bear the role of a diagnosis tools for several testicular and annex structures pathologies such as varicocele, testicular fibrosis and tumour (Pasha et al., 2010; Ali et al., 2014; Waheed et al., 2014; Kühn et al., 2016). All of the above proves that ultrasonography is a multi-faceted tool, showcasing its remarkable potential in reproductive assessment. However, in recent years, ultrasonography has revealed a new potential application, as several groups have explored the correlation between testicular parenchyma echogenicity and semen quality/fertility (England et al., 2017; Echegaray et al., 2018; Escartín et al., 2018; Lafuente et al., 2018; Muñoz et al., 2018; Ntemka et al., 2018). To enhance the precision of this correlation, several algorithms have been developed to provide an objective analysis of testicular echotexture in livestock animals (Echegaray et al., 2018; Escartín et al., 2018; Lafuente et al., 2018; Muñoz et al., 2018). ECOTEXT® is a digital image analysis of the testicular echotexture where each pixel of the ultrasound image represents a portion of the testicular parenchyma (Echegaray et al., 2018). The analysis attributes a numerical value to each tone of the grey scale presented by the pixels of the image, from black (0) to white (255). Next, it measures the distribution of black (EC1), white (EC2) and mean grey pixels (EC3) in a section of the testis with a known surface area (2.64 cm²). Finally, it analyses this information using algorithms, obtaining information on the density (density of hypoechoic areas), diameter (mean diameter of hypoechoic areas) and area (total percentage of hypoechoic area) (Echegaray et al., 2018; Escartín et al., 2018; Lafuente et al., 2018; Malo et al., 2018; Muñoz et al., 2018; Marcantonio, 2020). ECOTEXT® has been proven to predict fertility in bulls (Echegaray et al., 2018; Marcantonio, 2020), rams (Escartín et al., 2018), stallions (Lafuente et al., 2018) and boars (Muñoz et al., 2018) but was never studied in dromedary camels until now.

Testis always played a principal role in the evaluation of the male reproductive capacity. However, seminal plasma provides the environment for adequate sperm physiology and quality (nutrient, buffer, lubrication, sperm activation...) (Verze et al., 2016). Dromedary camels lack of seminal vesicles, therefore the vast majority of the ejaculate derives from prostatic and bulbourethral secretions (Hafez et al., 2001). The ultrasound visualization and measurement of accessory glands has previously been used a mean to predict fertility (Moxon et al., 2015).

Testosterone is a key male sex hormone playing a vital role in spermatogenesis (Tan et al., 2005). Testosterone has been related to various sperm parameters (Trussell et al., 2019) and is used as a biomarker for fertility in bulls (Kasimanickam et al., 2013).

Therefore, the aim of this study was to evaluate ability of standard and advanced BSE to differentiate between superior and inferior males. To do so the relationship between seminal parameters, fertility, testicular echotexture parameters, accessory glands volume and testosterone levels was characterized.

2. Materials and methods

Unless otherwise indicated, all chemicals were purchased from Sigma-Aldrich Co (St Louis, MO, USA). Green Buffer® (GB) was purchased from IMV (L'Aigle, France).

2.1. Experimental design

This study aimed to assess the effectiveness of standard and advanced BSE in distinguishing between superior and inferior males. The standard evaluation included clinical examination, testis volume assessment, and ultrasound evaluation of testicular parenchyma and epididymis. The advanced evaluation involved digital image analysis of

the testicular parenchyma, ultrasound examination of accessory glands, and measurement of total testosterone concentration.

The research was conducted through two experimental approaches: *in vitro* and *in vivo* experiments. In the *in vitro* experiment, diagnostic tools were evaluated using a group of camels trained for semen collection, referred to as the sperm group (n=11), enabling direct comparison with semen parameters. In the *in vivo* experiment, the same diagnostic tools were assessed using camels trained for natural mating, referred to as the natural mating group (n=15), to determine their predictive value for fertility. Both groups included camels classified as superior and inferior. Correlations, sensitivity, and specificity were analysed to determine the ability of each diagnostic tool to differentiate between superior and inferior males.

The group trained for semen collection is composed of camels from age 8–14 from the Camel Reproduction Centre (Dubai, UAE; 25°05'00.2 N 55°32'23.0E). Three ejaculates were obtained from each male using an artificial vagina as described by Skidmore et al. (2018), during the breeding season (November to April). Ejaculates were immediately transported to the laboratory and placed in a 37°C water bath. All animal procedures were approved by the Animal Care and Use Committee of the Camel Reproduction Center. The group trained for natural mating is composed of camels (8–18 years old) from a milk production factory.

All diagnostic methods and image processing were conducted by the same practitioner, under identical experimental conditions, and in strict adherence to ethical guidelines.

2.2. Semen assessment

Macroscopic evaluation of the ejaculate (volume and colour) was performed immediately after collection. The volume was measured directly from the graduated collecting tube (Malo et al., 2017). The colour (varying from creamy white, milky white to translucent greyish white) was assessed by subjective visual inspection of the semen sample (Skidmore et al., 2013; Al-Bulushi et al., 2018). The sample was then diluted using Tris-citrate-fructose buffer medium (TCF, pH = 6.9), supplemented with bovine serum albumin (0.05 %, w/v), EDTA (10 mM) and 4 % egg yolk. Liquefaction was obtained by gentle pipetting with a plastic pipette (20 min) (Malo et al., 2017; Swelum et al., 2019).

Once the sample was liquefied, sperm concentration, motility, kinematic parameters, morphology, vitality, acrosome integrity and mitochondrial functionality were assessed.

2.2.1. Motility parameters

Motility and kinematic parameters were analysed by CASA system (Ceros II®, Hamilton Thorne, MA, USA). Diluted samples (3 µL) were placed in a counting chamber (MicroTool™, Cytonix, USA), and a total of 1000 sperm cells were analysed. Total and progressive motility (%) as well as kinematic parameters were recorded. The kinematic parameters were: average path velocity (VAP; µm/s), straight line velocity (VSL; µm/s), curvilinear velocity (VCL; µm/s), amplitude of lateral head displacement (ALH; µm), beat cross frequency (BCF; %), straightness (STR; %) and linearity (LIN; %).

2.2.2. Morphology

The morphology was evaluated by eosin-nigrosin staining (5 % eosin, 10 % nigrosin diluted in 0.1 M citrate solution) (Malo et al., 2017). In total, 200 cells were evaluated under bright field microscopy at 100x (Olympus BX53F, No fluorescence filter, Olympus, Tokyo, Japan). Abnormal heads (large, small, conical, pyriform, vacuolated, double head), and midpieces (irregular, abnormally thick/thin), and presence of cytoplasmic droplets and abnormal tails (short, multiple, broken, coiled, absent, bent) were counted to describe the abnormal sperm cell morphology.

2.2.3. Assessment by fluorescence

Vitality, acrosome integrity and mitochondria functionality were assessed using a fluorescence microscope (Olympus BX53F, Olympus, Tokyo, Japan) at 100x. A total of 200 sperm cells were counted per sample for each parameter.

The vitality was assessed using SYBR-14 and propidium iodide staining (L-7011, Live/Dead Sperm Viability Kit; Molecular Probes Europe, Leiden, The Netherlands), according to the manufacturer's instructions and the protocol described by Garner et al. (1997). Sperm were then observed under TRITC Filter (Emission: 570–613 nm, Excitation: 532–554 nm). Based on the integrity of the plasma membrane sperms were classified as intact (alive; green head) or damaged (dead; red head).

The acrosome integrity was evaluated using fluorescein isothiocyanate conjugated with peanut lectin from *Arachis hypogaea* (FITC-PNA) staining as described by Malo et al. (2019) with slight modifications. Briefly, 30 μ L of seminal sample were diluted with 140 μ L of GB and fixed with 2 μ L of 4 % paraformaldehyde. Permeabilization was performed using 1 % Nonidet P40. Later, 6 μ L of FITC-PNA solution (2 mg/mL) was added to stain for 30 min. Sperm were then evaluated under FITC Filter (Emission: 513–556 nm, Excitation: 467–498 nm). Based on the integrity of the outer acrosomal membrane, they were classified into intact acrosome (intense, uniform fluorescence over the acrosomal cap) or damaged acrosome (no fluorescence or not uniform fluorescence or vesiculated acrosomal membrane) (Almadaly et al., 2012).

Finally, the mitochondrial functionality was assessed using Rhodamine 123 (R123) staining as described by Eskandari and Momeni (2016) with slight modifications. Briefly, 30 μ L of sample were diluted with 140 μ L of GB and 5 μ L of R123 solution (1 mg/mL). The solution was incubated protected from the light at room temperature for 30 min. Subsequently, the solution was centrifuged at 600 g for 20 min. The supernatant was removed and the pellet was resuspended in 140 μ L GB and 2 μ L of 4 % paraformaldehyde were added. Sperm were then evaluated under FITC Filter and classified as having active mitochondria (green midpieces) or inactive mitochondria (no colour).

2.3. Standard breeding soundness evaluation

Animals from each group were submitted to general physical examination and testis measurements. Due to the testis' position in camels, average testis volume was calculated using the following formula (Hsieh et al., 2009):

$$\text{Average testis volume}(cm^3) = \text{lenght} \times \text{width}^2 \times \left(\frac{\pi}{6}\right)$$

For the ultrasound examination, the animals were placed in sternal recumbency with their legs tied. The images were taken using the EXAGO® ultrasound machine (ECM, Angulemme, France) connected to a multifrequency linear probe (5–10 MHz) set at 7.5 MHz. It consisted of transverse and longitudinal sections of both testicles as well as the head and tail of the epididymis. Animals were then classified into apparently normal (Fig. 2A) and abnormal parenchyma (Fig. 2B, C) according to naked eye assessment of the ultrasound images. Normal parenchyma was defined as homogeneous mildly coarse echogenicity surrounded by an echogenic outline (tunica albuginea) and centre (testicular mediastinum) (Waheed et al., 2014). The head (Fig. 2D) and tail (Fig. 2E) of the epididymis was defined as triangular structure, slightly hyperechoic, localized cranially and caudally to the testis, respectively. The sensitivity and specificity of the naked eye ultrasound evaluation was calculated.

2.4. Advanced breeding soundness evaluation

The advanced BSE consisted of digital ultrasound image analysis, accessory glands exploration and total serum testosterone

concentration. Correlations, sensitivity and specificity were then calculated.

For the digital ultrasound image analysis, the scanner was configured to obtain images in I-mag format (image format that allows ECOTEXT® analysis) with total gain 0, focus at 2 cm, depth of 6 cm. Three transverse ultrasounds were performed per testicle of the caudal, middle and cranial testicular parenchyma. The images were then analysed using the ECOTEXT® software. The analysis was performed on a fixed square (2.64 cm²) of parenchyma ventral to the mediastinum and dorsal to the tunica albuginea. Three parameters were analysed in normal: black (EC1), white (EC2) and mean grey (EC3) pixels. In addition, three parameters were analysed in high resolution: density of hypoechoic areas (density), total percentage of hypoechoic area (area) and mean diameter of hypoechoic areas (diameter). The reference values used to identify normal parenchyma consisted of: EC1 (1 < EC1 < 500), EC2 (≤ 30), EC3 (70 < EC3 < 100), total percentage of hypoechoic area (5–50 %), mean diameter of hypoechoic areas (90–150 μ m) and density of hypoechoic areas ($\geq 155/cm^2$), (Echegaray et al., 2018; Escartín et al., 2018; Lafuente et al., 2018; Malo et al., 2018; Muñoz et al., 2018; Marcantonio, 2020).

For the accessory glands exploration, the images were taken using the EXAGO® ultrasound machine (ECM, Angulemme, France) connected to a multifrequency intrarectal linear probe set at 7.5 MHz. The probe was positioned looking ventrally. The prostate gland was found caudally to the urinary bladder as a homogeneous mildly coarse oval shape. The bulbourethral glands were found caudally to the prostate as a homogeneous mildly coarse round shape. Measurement of the length and width of each gland was taken. The volume for each gland was calculated based of the following formulas:

$$\text{Prostate volume}(cm^3) = \text{lenght} \times \text{width}^2 \times 0.56$$

(Mitterberger et al., 2010)

$$\text{Bulbourethral volume}(cm^3) = \left(\frac{\text{Width}}{2}\right)^3 \times \left(\frac{4}{3}\right)\pi$$

(Camela et al., 2017)

Total testosterone serum concentration was measured by electrochemiluminescence Immunoassay (ECLIA) based on a competitive test principle using a high-affinity monoclonal antibody (sheep) specifically directed against testosterone. Samples were all collected in the morning at fixed time.

2.5. Statistical analysis

Statistical analysis was performed using GraphPad Prism 8 software. First, in the sperm group, the mean value of the 3 ejaculates was calculated for each seminal parameter. In the natural mating group, the fertility percentage [(number of pregnancy/number of mating) x 100] was calculated. For the standard BSE, the sensitivity and specificity of the naked eye ultrasound analysis were calculated using Fisher's exact test and the following formula:

$$\text{Sensitivity} = \frac{\text{superior males presenting normal parenchyma at the naked eye ultrasound analysis}}{\text{superior males}}$$

$$\text{Specificity} = \frac{\text{inferior males presenting abnormal parenchyma at the naked eye ultrasound analysis}}{\text{inferior males}}$$

Superior males are males that either present high motility (*in vitro* experiments) or a fertile (*in vivo* experiments). Inferior males are males that either present low motility (*in vitro* experiments) or a subfertile (*in vivo* experiments). High motility was defined as total motility ≥ 35 % and low motility as total motility < 35 %. Fertile males were defined as fertility ≥ 40 % and subfertile as fertility < 40 %.

Subsequently, for the advanced BSE, a statistical analysis (Student's

t-test for independent samples) of the values of the six ECOTEXT® ultrasound parameters were performed to determine if there were differences between testes (left and right). A bivariate correlation analysis was carried out between the ECOTEXT® variables, accessory glands volume, testosterone and seminal parameters or fertility percentage (Spearman's test). Statistical tests were considered as significant for P values below 0.05. Correlation coefficient (Spearman R) between 0.3 and 0.49 were considered moderate and higher than 0.5 strong (Agresti, 2018). Sensitivity and specificity of each of the factors evaluated during the advanced BSE were assessed using the following formula:

$$\text{Sensitivity} = \frac{\text{superior males presenting positive test}}{\text{superior males}}$$

$$\text{Specificity} = \frac{\text{inferior males presenting negative test}}{\text{inferior males}}$$

All average results are presented in mean ± standard deviation.

3. Results

3.1. In vitro experiments

3.1.1. Semen analysis

The average value of each of the seminal parameters for each male of the sperm group are summarized in Table 1. In the sperm group, 6 camel bulls presented a total motility higher than 35 % (superior males), 5 camel bulls presented a total motility lower than 35 % (inferior males). The highest motility was 56.6 %.

3.1.2. Standard breeding soundness evaluation

All animals presented adequate physical conditions for breeding. The

results of the standard BSE are summarized in Table 2. There was no statistical difference in testis volume between superior and inferior males (Fig. 1A). No correlations between testis volume and any parameters studied were found. Interestingly, 9 animals appeared to have a normal testicular parenchyma (Figs. 2A), 1 male showed a hyperechoic parenchyma (Fig. 2B) and another showed hypoechoic parenchyma (Fig. 2C). The naked eye ultrasound evaluation obtained a sensitivity of 100 % and a specificity of 20 %, meaning it was very successful in detecting superior males (high motility) but not in distinguishing inferior ones (low motility).

3.1.3. Advanced breeding soundness evaluation

Given the results from the standard BSE obtaining low specificity, advanced BSE was performed to evaluate if another diagnostic tool presented higher specificity. For the digital ultrasound image analysis, the semen group showed average EC1 (94 ± 232), EC2 (122 ± 339), EC3 (87 ± 22), density (139 ± 38 /cm²), diameter (174 ± 210 μm) and area (18 ± 15 %) (Table 2). Correlations between echotexture parameters with seminal parameters are summarized in Table 3. Among the correlations, EC2 showed strong correlation with vitality, mitochondria potential and head defect. EC3 showed strong correlation with ejaculate volume, vitality and mitochondria potential. Area showed strong correlation with vitality and head defects. Finally, density showed a strong correlation with vitality and mitochondria potential. The sensitivity and specificity of each one of the echotexture parameters can be found in Table 4. Although most echotexture parameters presented strong correlations, when studying the contingency of the parameters, only EC2 reach statistical significance, presenting a sensitivity of 86 % and a specificity of 100 % in the sperm group.

Bulbourethral (Fig. 2F) and prostate (Fig. 2G) glands were successfully identified in all animals. The average prostate and bulbourethral

Table 1
Seminal parameters obtained in the *in vitro* experiments (Mean ± SD) (n=11).

	Dromedary camel											Population Mean ± SD
	1	2	3	4	5	6	7	8	9	10	11	
Vol	4.3 ±1.9	4.0 ±1.2	7.2 ±0.9	3.2 ±0.4	2.5±0.6	6.0 ±2.0	6.7 ±1.3	3.3 ±1.2	3.2 ±0.9	1.3 ±0.5	3.2±0.8	4.1 ±0.5
Conc	338 ±154	621 ±178	259 ±58	344 ±146	116±79	144 ±39	192 ±99	169 ±84	233 ±45	592 ±312	187.5 ±162	388 ±87
TM	35.1 ±12.0	52.7 ±6.2	40.0 ±11.6	55.5 ±9.2	38.1 ±26.2	56.6 ±10.8	19.9 ±11.8	22.8 ±11.4	19.2 ±12.4	29.2 ±13.9	15.6 ±19.2	38.0 ±3.9
PM	20.3 ±7.5	28.5 ±3.2	27.5 ±7.1	35.0 ±4.0	25.8 ±18.8	30.4 ±4.6	15.6 ±9.4	15.2 ±7.7	9.8 ±4.9	16.6 ±7.9	11.3 ±14.4	23.3 ±2.3
VAP	50.3 ±13.1	70.8 ±5.8	69.6 ±5.5	56.5 ±6.9	34.3 ±23.8	77.0 ±7.8	39.6 ±19.9	41.1 ±20.7	44.2 ±6.4	54.3 ±12.5	34.4 ±32.5	57.2 ±3.9
VSL	33.6 ±7.9	37.3 ±3.0	43.6 ±2.1	33.6 ±2.1	22.7 ±15.5	42.5 ±1.0	28.3 ±14.2	25.3 ±12.6	26.8 ±2.9	30.8 ±6.5	21.5 ±20.7	34.5 ±2.2
VCL	128.6 ±38.7	179.9 ±14.8	173.5 ±11.5	130.6 ±18.0	84.6 ±59.9	203.6 ±11.6	99.97 ±50.0	99.8 ±50.6	110.6 ±22.8	138.7 ±30.6	90.4 ±85.8	144.1 ±10.2
LIN	33.2 ±4.8	23.1 ±0.3	27.8 ±1.7	29.7 ±4.3	22.1 ±15.2	23.2 ±1.4	19.6 ±9.8	17.9 ±9.0	26.6 ±4.5	23.1 ±0.8	16.4 ±14.2	25.2 ±1.5
STR	70.9 ±3.3	55.7 ±0.5	64.1 ±2.3	61.8 ±4.6	50.6 ±34	58.6 ±4.9	471.1 ±23.5	42.1 ±21.1	59.0 ±6.5	57.3 ±1.9	41.1 ±35.6	58.2 ±3.1
ALH	7.1 ±1.7	9.7 ±0.6	9.7 ±0.6	7.9 ±0.6	5.0±3.6	10.2 ±0.4	5.5 ±2.7	5.7 ±2.8	6.4 ±1.3	8.1 ±1.3	5.2±4.9	8.0 ±0.5
BCF	23.9 ±1.4	26.4 ±1.4	24.1 ±1.7	22.9 ±0.5	17.3 ±11.7	24.1 ±1.6	16.2 ±8.1	15.1 ±7.5	40.2 ±17.2	25.2 ±1.6	18.1 ±18.2	24.1 ±2.1
Vit	58.3 ±5.3	63.3 ±4.9	44.0 ±4.7	59.3 ±12.0	47.5 ±31.9	64.3 ±9.4	49.7 ±9.0	41.7 ±9.0	40.7 ±12.3	50.3 ±9.0	32.3 ±18.2	53.6 ±2.8
IA	84.0 ±1.2	79.7 ±7.4	71.3 ±11.9	84.7 ±3.0	51.8 ±34.8	84.3 ±3.9	79.0 ±5.2	86.0 ±2.6	70.3 ±15.7	73.7 ±13.3	47.7 ±24.4	78.9 ±2.5
MA	10.3 ±3.8	11.7 ±2.7	16.0 ±2.1	9.0 ±1.7	16.8 ±11.6	6.3 ±1.5	16.3 ±0.9	14.7 ±1.9	15.0 ±1.2	16.7 ±3.9	22.7 ±11.8	12.9 ±0.9
AH	3.3 ±1.3	4.3 ±1.2	6.0 ±2.3	7.0 ±1.2	10±10	2.7 ±1.5	8.3 ±2.2	8.3 ±0.7	6.3 ±3.0	8.3 ±2.2	9.7±6	5.6 ±0.6
Mit	64.3 ±17.8	64.7 ±4.3	46.3 ±10.5	46.3 ±19.1	43.3 ±29	70.3 ±5.2	34.3 ±14.7	41.0 ±8.2	35.0 ±18.8	34.3 ±14.7	31.7 ±21.5	50.5 ±4.1

Animals 1–6 were considered as high motility while animals 7–11 were considered as low motility. Vol: Volume (mL); Visc: Viscosity (1–5); Conc: Concentration (×10⁶/mL); TM: Total motility (%); PM: Progressive motility (%); VAP: Average path velocity (μm/s); VSL: Straight line velocity (μm/s); VCL: Curvilinear velocity (μm/s); LIN: linearity (%); STR: straightness (%); ALH: Amplitude of lateral head displacement (μm); BCF: Beat cross frequency (Hz); Vit: Vitality (%); IA: Intact acrosome (%); MA: Morphology abnormal (%); AH: Abnormal head (%); Mit: Functioning mitochondria (%).

Table 2
Breeding soundness evaluation results in the *in vitro* experiments (n=11).

Dromedary Camel	Standard breeding soundness evaluation					Advanced breeding soundness evaluation							Testosterone
	Testis volume	Echography findings			Digital parenchyma analysis			Accessory glands volume					
		Testicular parenchyma	Epididymis		EC1	EC2	EC3	Area	Diameter	Density	Prostate	Bulbourethral	
			Head	Tail									
1	RT 131	N	N	N	74	4	83	18	131	153	6.6	1.3	214.9
	LT 171	N	N	N	39	0	73	20	151	140			
2	RT 117	N	N	N	3	30	93	11	101	160	13.3	1.0	183.3
	LT 131	N	N	N	2	64	100	9	91	158			
3	RT 92	N	N	N	28	2	76	18	136	156	9.2	1.4	153.3
	LT 88	N	N	N	9	8	87	11	104	159			
4	RT 157	N	N	N	479	0	50	47	393	63	10.6	1.1	45.4
	LT 177	N	N	N	Not evaluable								
5	RT 62	F	N	N	0	1564	135	4	60	113	58.6	0.8	143.2
	LT 308	N	N	N	2	131	103	10	96	169			
6	RT 63	N	N	N	31	60	92	13	113	155	11.4	1.5	232.1
	LT 6	N	N	N	0	24	92	12	113	157			
7	RT 77	N	Adh	N	13	17	89	13	104	165	10.9	0.9	298.1
	LT 77	N	N	N	12	220	106	9	90	150			
8	RT 109	N	N	N	12	2	74	18	139	150	10.1	0.8	150.4
	LT 129	N	N	N	40	0	75	18	143	149			
9	RT 184	N	N	N	6	27	93	12	103	163	8.6	1.0	252.4
	LT 365	N	N	N	0	20	96	6	78	154			
10	RT 174	N	NF	N	0	281	108	8	87	159	8.3	0.7	5.7
	LT 176	N	NF	N	0	110	106	7	82	146			
11	RT 154	D	NF	NF	977	0	40	67	1020	21	6.1	1.0	376.3
	LT 184	D	NF	NF	255	0	53	38	327	87			
Average ± SD	142 ± 79				94 ± 232	122 ± 339	87 ± 22	18 ± 15	174 ± 210	139 ± 38	14.0 ± 14.9	1 ± 0.3	186.8 ± 106.1

Animals 1–6 were considered as high motility while animals 7–11 were considered as low motility. RT: Right testis; LT: Left testis; N: normal; D: Dark parenchyma (Hypoechoic); F: Fibrosis (Hyperechoic); NF: Not found; Adh: Adhesions; EC1: black pixels; EC2: white pixels; EC3: mean grey pixels; Area: total percentage of hypoechoic area (%); Diameter: Diameter of hypoechoic areas (µm); Density: Density of hypoechoic areas/cm²; Volume (cm³). Testosterone (µg/dl).

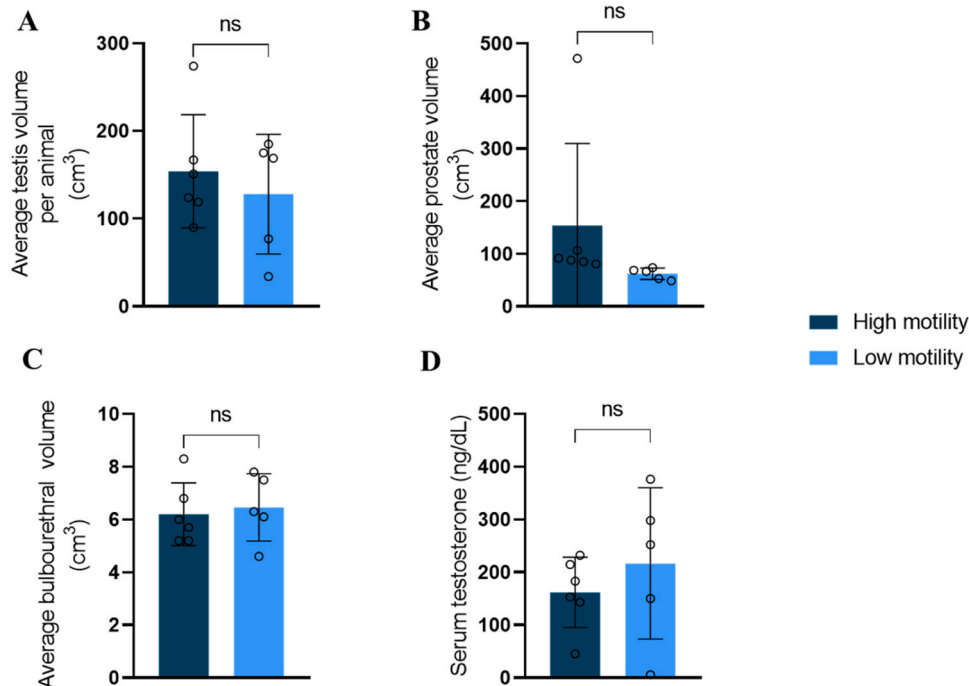


Fig. 1. Testis (A), Prostate gland (B), Bulbourethral glands (C) volume and serum testosterone concentration (D) in the *in vitro* study (n = 11).

volume in the sperm group were $14.0 \pm 14.9 \text{ cm}^3$ and $1.0 \pm 0.3 \text{ cm}^3$, respectively (Table 2). No statistical differences were found between any of the groups (Fig. 1B and C). However, strong correlation between bulbourethral and ejaculate volume were found (Table 3).

Testosterone concentration of each animal can be found in Table 2.

No statistical difference between the groups was observed (Fig. 1D) and no correlation was found.

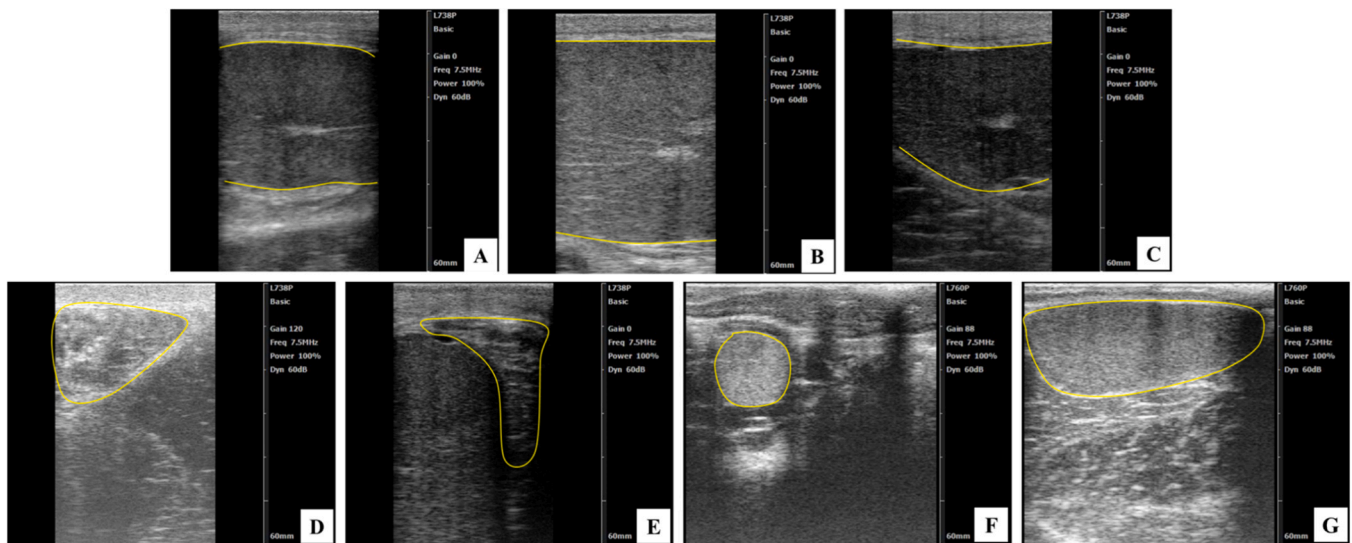


Fig. 2. Ultrasound images of the camel bull reproductive tract: Normal (A), Hyperechoic (B), Hypoechoic (C) Testicular Parenchyma, Head (D) and Tail (E) of Epididymis, Bulbourethral gland (F) and prostate (G). The organ of interest of each image has been encircled by a yellow line.

Table 3
Correlation analysis between seminal parameters and advanced breeding soundness evaluation variables in the *in vitro* experiments (n=11).

	Pearson correlation coefficients						
	Ejaculate volume	Sperm concentration	Total motility	Progressive motility	Vitality	Mitochondria potential	Head defect
EC1					0.46*	0.48*	-0.44*
EC2	-0.49*		-0.49*		-0.50*	-0.59**	0.61**
EC3	-0.51*		-0.48*		-0.55**	-0.60**	0.47*
Area					0.52*	0.48*	-0.50*
Diameter					0.49*	0.46*	
Density					-0.50*	-0.54**	
Bulbourethral volume	0.63*						

Only the relevant and significant correlations are shown in the present table. EC1: black pixels; EC2: white pixels; EC3: mean grey pixels; Area: total percentage of hypoechoic area (%); Diameter: Diameter of hypoechoic areas (µm); *: 0.05 < P < 0.01; **: 0.01 ≥ P; Light gray: Correlation coefficient (Spearman R) between 0.3 and 0.49 were considered moderate while values higher or equal to 0.5 were considered strong.

Table 4
Sensitivity and specificity of the digital ultrasound image analysis in the *in vitro* experiments (n=11).

	Sperm	
	Sensitivity	Specificity
EC1	1	0.33
EC2	0.86*	1*
EC3	0.86	0.33
Area	1	0.33
Diameter	0.86	0.33
Density	0.57	0.33

EC1: black pixels; EC2: white pixels; EC3: mean grey pixels; Area: total percentage of hypoechoic area (%); Diameter: Diameter of hypoechoic areas (µm).

Table 5
Fertility presented in the *in vivo* experiments (n=15).

	Dromedary camels														Population Mean ± SD	
	1	2	3	4	5	6	7	8	9	10	11	12	13	14		15
Fertility (%)	47.4	55.7	41.8	44.8	64.4	55.8	43.2	47.4	26.7	36.6	37.7	39.7	5.4	31.8	2	38.7 ± 17

Animals 1-8 were considered fertile while animals 9-15 were considered subfertile.

3.2. In vivo experiments

3.2.1. Fertility of males

The values of fertility for each male are summarized in Table 5. Among the 15 males, 8 presented a fertility higher than 40 % (superior males), therefore were considered fertile, and 7 presented a fertility lower than 40 % (inferior males). The highest fertility was 64.4 %.

3.2.2. Standard breeding soundness evaluation

All males presented adequate physical conditions for breeding. The results of the standard BSE are summarized in Table 6. There was no statistical difference in testis volume between superior and inferior males (Fig. 3A). Interestingly, 9 animals appeared to have a normal testicular parenchyma (Fig. 2A), 3 males showed a hyperechoic parenchyma (Fig. 2B). The naked eye ultrasound evaluation obtained a sensitivity of 75 % and a specificity of 14 %, meaning it was successful in detecting superior males with high fertility but not in distinguishing inferior ones with low fertility.

Table 6
Breeding soundness evaluation results in the *in vivo* experiments (n=15).

Camel	Standard breeding soundness evaluation					Advanced breeding soundness evaluation							Testosterone	
	Testis volume	Echography findings			Digital parenchyma analysis			Accessory glands		Testosterone				
		Testicular parenchyma	Epididymis		EC1	EC2	EC3	Area	Diameter		Density	Volume		
			Head	Tail								Prostate	Bulbourethral	
1	RT 200	N	N	N	1	0	66	14	123	169	8.5	3.9	41	
	LT 189	N	N	N	1	0	76	13	112	164				
2	RT 230	N	N	N	6	22	93	11	98	165	11.2	2.7	10	
	LT 189	N	N	N	49	0	64	19	149	157				
3	RT 507	F	N	N	Not evaluable									
	LT 449	F	F	F										
4	RT 317	N	N	N	4	85	101	10	97	159	6.7	1.9	32	
	LT 241	N	N	N	31	25	92	14	114	165				
5	RT 266	N	N	N	0	1	86	10	95	175	14.7	3.1	26	
	LT 225	N	N	N	7	68	98	12	107	155				
6	RT 326	F	Inc	N	Not evaluable									
	LT 319	F	Inc	N										
7	RT 357	N	N	N	6	42	91	10	99	158	20.0	3.3	17	
	LT 317	N	N	N	4	0	79	15	114	168				
8	RT 329	N	N	N	1	376	110	7	84	147	10.2	4.2	16	
	LT 230	N	N	N	13	135	96	12	107	162				
9	RT 339	N	Inc	Inc	0	41	99	8	82	157	13.0	2.2	129	
	LT 99	N	Inc	Inc	Not evaluable									
10	RT 459	N	N	N	10	141	99	12	100	159	9.9	3.2	43	
	LT 459	N	N	N	2	85	101	9	89	159				
11	RT 449	N	N	N	4	34	97	11	100	149	11.5	3.0	162	
	LT 395	N	N	N	8	130	100	10	97	157				
12	RT 189	N	N	N	7	27	96	11	102	162	8.2	2.2	2	
	LT 197	N	N	N	7	27	96	11	102	162				
13	RT 674	N	N	N	4	241	106	9	91	161	11.2	3.2	128	
	LT 410	N	N	N	0	243	110	6	74	144				
14	RT 253	F	N	N	Not evaluable									
	LT 337	F	N	N										
15	RT 125	N	Inc	N	8	85	97	11	99	165	5.6	3.0	2	
	LT 140	N	Inc	N	7	0	76	12	104	153				
Average		307 ±			8 ±	79 ±	92 ±	11 ±	102 ±15	160 ± 7	10.9 ±	3.0 ± 0.7	11 ±3.8	
± SD		129			11	96	13	3			3.8			

Animals 1–8 were considered fertile while animals 9–15 were considered subfertile. RT: Right testis; LT: Left testis; N: normal; D: Dark parenchyma (Hypoechoic); F: Fibrosis (Hyperechoic); NF: Not found; Adh: Adhesions; Inc: Increased in size; EC1: black pixels; EC2: white pixels; EC3: mean grey pixels; Area: total percentage of hypoechoic area (%); Diameter: Diameter of hypoechoic areas (μm); Density: Density of hypoechoic areas/ cm^2 ; Volume (cm^3). Testosterone ($\mu\text{g}/\text{dl}$).

3.2.3. Advanced breeding soundness evaluation

Given the results from the standard BSE obtaining low specificity, advanced BSE was performed to evaluate if another diagnostic tool presented higher specificity. For the digital ultrasound image analysis, the fertility group showed average EC1 (8 ± 11), EC2 (79 ± 96), EC3 (92 ± 13), density ($160 \pm 7/\text{cm}^2$), diameter ($102 \pm 15\mu\text{m}$) and area ($11 \pm 3\%$) (Table 6). Correlations between echotexture parameters and fertility were studied. A significant negative correlation between fertility and EC3 ($R = -0.78$; $P < 0.05$), and significant positive correlation between fertility and diameter of hypoechoic area ($R = 0.70$; $P < 0.01$), or density ($R = 0.75$; $P < 0.001$). Although most echotexture parameters presented strong correlations, when studying the contingency of the parameters, none showed statistical significance.

Bulbourethral (Fig. 2F) and prostate (Fig. 2G) glands were successfully identified in all animals. The average prostate and bulbourethral volume in the fertility group were $10.9 \pm 3.8 \text{ cm}^3$ and $3.0 \pm 0.7 \text{ cm}^3$, respectively (Table 6). No statistical differences were found between any of the groups (Fig. 3B and C).

Testosterone concentration of each animal is in Table 6. No statistical differences between the groups were observed (Fig. 3D) and no correlations were found.

4. Discussion

Compared to other species, dromedary camel males exhibit low reproductive efficiency, likely stemming from their poor semen quality characterized by highly viscous ejaculate, low volume and sperm concentration (Rateb, 2006; Malo et al., 2017). Previous reports have

revealed a noteworthy percentage of subfertile males within the population (Rateb, 2006). Consequently, the prediction of male fertility and diagnosis of subfertility in dromedary camels are essential to enhance the outcome of both natural service and assisted breeding (Nicholas, 1996; Rated, 2006).

The standard BSE is composed of physical examination, testis measurement and ultrasound testicular parenchyma evaluation (Waheed et al., 2014). In the present study, we noted that the measurement of testis volume did not serve a predictive factor of the male's reproductive capacity, as it lacks correlations with any of the factors studied. This aligns with prior study (Waheed et al., 2014) which similarly reported no significant differences between testis size in fertile and infertile camels. While these results may appear unexpected, considering that testis volume is a reliable predictor of fertility in other species (Thompson et al., 1979; Perumal, 2014), we hypothesize that the unique location and angle of camels' testes (Hafez and Hafez, 2001) present challenges in obtaining precise measurements. This could potentially account for the observed lack of correlation with the studied parameters. Subsequently, the ultrasound evaluation consisted of the visualization of testicular parenchyma and epididymis. We successfully obtained for the first time, images of epididymal head and tail. Because of the camels' testis position, the head of the epididymis is usually difficult to reach (Waheed et al., 2014). Nevertheless, we were successful by positioning the probe in a 45 cranio-caudal angle on the cranial part of the testis while applying slight pressure. The "naked eye" ultrasound image evaluation obtained a sensitivity of 100 % and a specificity of 20 % or 14 %, meaning it was very successful in detecting superior males but not in distinguishing inferior ones. We concluded that the standard BSE was

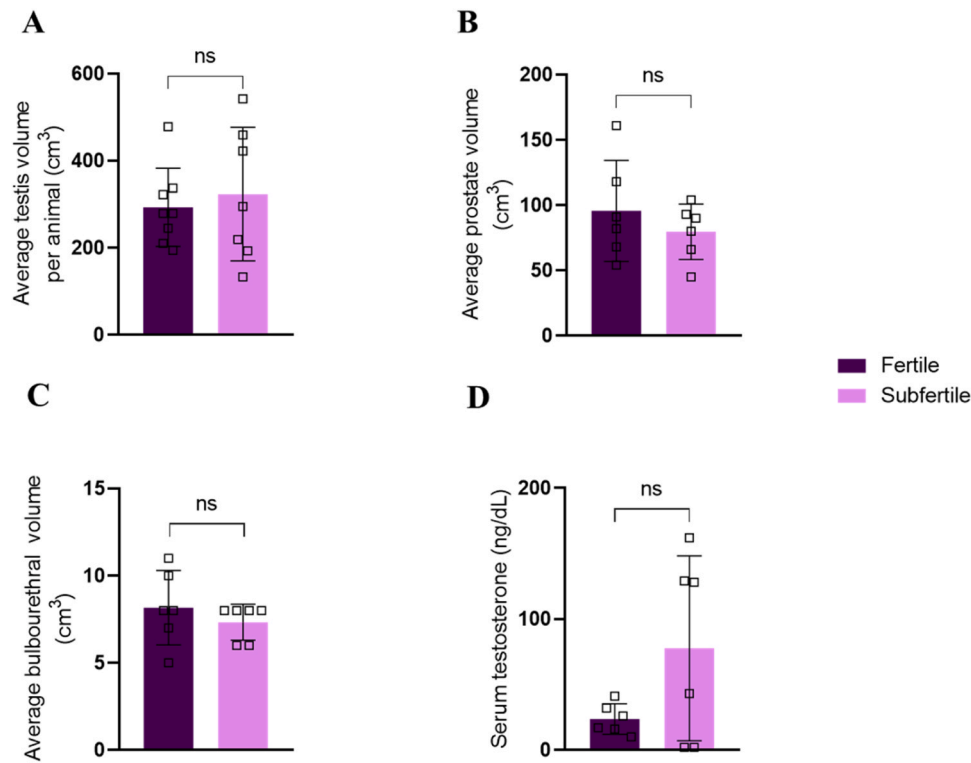


Fig. 3. Testis (A), Prostate gland (B), Bulbourethral glands (C) volume and serum testosterone concentration (D) in the *in vivo* study ($n = 15$).

not successful in detecting subfertility in camels. Therefore, an advanced BSE is needed and novel diagnostic tools need to be studied.

The first diagnostic tool tested was the digital analysis of testicular parenchyma echotexture. Given the inherent limitations of visual analysis in ultrasonograms (Kastelic and Brito, 2012), which relies on the human eye capable of discerning only 30 shades of grey (Kreit et al., 2013), while ultrasound images can show up to 256 shades of grey, we hypothesized that a digital objective analysis would allow a more precise description of the testicular parenchyma. Our results are promising as, when performing *in vitro* studies, various echotexture parameters correlate with several of the seminal parameters. Based on these correlations, a more echogenic parenchyma presents fewer morphologically normal alive sperm, which agrees with previous work in dogs (Moxon et al., 2015), rams (Escartín et al., 2018), boars (Muñoz et al., 2018) and stallions (Lafuente et al., 2018). In addition, this is in concordance with the physiology of the testis as sperm morphogenesis, especially of the head takes place in the seminiferous tubules (Hess and Renato de Franca, 2008). Previous studies applying digital image analysis in other species (Echegaray et al., 2018; Escartín et al., 2018; Lafuente et al., 2018; Malo et al., 2018; Muñoz et al., 2018; Marcantonio, 2020) have only mentioned the relationship between echotexture parameters, vitality and morphological abnormalities. However, in the present study, based on the correlations observed, a less echogenic parenchyma correlates with a higher number of functional mitochondria. Unfortunately, there is no clear relation between parenchymal echotexture and mitochondrial membrane potential in the literature. However, we can contemplate several hypotheses to explain these correlations. During the spermatogenesis, there is a swelling of intra-cristal space and a flattening of the matrix against the outer membrane cause the mitochondria to condense inside the midpiece (De Martino et al., 1979). Our results suggest, at least to some extent, that a malformation of the midpiece during spermatogenesis caused by a testicular injury can affect the mitochondrial membrane potential and consequently the sperm motility. This agrees with Pelliccione et al. (2011) findings where the majority of mitochondria in abnormal midpieces (defect of

spermatogenesis) showed swollen intermembrane spaces and scattered disorganized cristae. Furthermore, authors described men with abnormalities in the mitochondria also showed altered Sertoli cell mitochondria (Folgerø et al., 1993), which links the mitochondrial condition to the state of the testicular parenchyma. Among the echotexture parameters, EC2 (white pixels) and EC3 (mean level of grey) presented the highest and strongest correlations. However, when submitted to a contingency study, only EC2 (white pixels) presented strong sensitivity (86 %) and specificity (100 %). We therefore conclude that among the echotexture parameters analyzed through digital analysis, EC2 (white pixels) is a strong marker for sperm quality. Interestingly, when performing *in vivo* studies, with other males trained for natural mating, based on the correlation found a less echogenic parenchyma correlates with a higher fertility. However, when submitted to a contingency study, none of the echotexture parameters presented statistically significant results. We therefore conclude that among the echotexture parameters analyzed through digital analysis, EC2 (white pixels) is a strong marker for sperm quality but none of the echotexture parameters can predict fertility. Due to challenges in animal management, this study could not simultaneously assess semen quality, fertility, and echotexture parameters within the same animal population. However, conducting such an integrated analysis would be of significant interest for future research.

The mean to assess fertility visualization and measurement of the accessory glands has been employed by (Moxon et al., 2015) given their crucial role in creating the necessary conditions for male fertility (Verze et al., 2016). Dromedary camels lack of seminal vesicles, consequently the vast majority of the ejaculate derives from prostatic and bulbourethral secretions (Hafez and Hafez, 2001). We report for the first time in dromedary camels, images of the prostate and bulbourethral glands acquired through transrectal ultrasound. Interestingly, we found a robust correlation between ejaculate volume and bulbourethral volume, rather than prostate volume. Therefore, we hypothesize that in dromedary camels, bulbourethral glands play a predominant role in the secretion of accessory glands, making up the vast majority of the ejaculate volume. This is in accordance with the high viscosity of camels'

ejaculates, as bulbourethral glands are known to secrete an alkaline mucus-like fluid (Johnson et al., 2010). Considering all of the above, we conclude that the examination of accessory glands, along with their measurements, are valuable parameters to predict the sperm quality in dromedary bull. Further studies involving larger populations are needed to establish threshold values of volume in those two glands, therefore allowing sensitivity and specificity studies.

Testosterone concentration showed no significant difference between the groups and no correlations were found with any of the parameters studied. These findings are surprising as testosterone plays a major role in spermatogenesis (Zhang et al., 2018) and is considered a fertility marker in bull (Kasimanickam et al., 2013) and buffalo bull (Almadaly et al., 2023). Nonetheless, it is crucial to acknowledge that measuring testosterone levels addresses one facet of male fertility and that other pathologies (obstruction, infection, accessory glands inflammation) can alter male fertility without altering serum testosterone level (Skakkebaek et al., 2016; Zhang et al., 2018). Furthermore, in the present study, we measured total testosterone concentration but only free testosterone has biological effect (Laurent et al., 2016); discrepancies may exist between the total and free testosterone, highlighting the importance of measuring free testosterone for more precise information. Therefore, we conclude that total testosterone concentration does not allow the prediction of fertility in dromedary camels.

5. Conclusions

In conclusion, the utilization of standard BSE evaluation and additional tests such as digital ultrasound image analysis and measurement of accessory glands (prostate and bulbourethral glands), proved to be informative. Notably, assessing levels of white pixels through digital image analysis showed high sensitivity and specificity in the evaluation of semen quality in dromedary camels. Furthermore, bulbourethral glands volume correlated with ejaculate volume and fertility, underscoring the pivotal role of bulbourethral glands in the composition of dromedary camels' ejaculate. The above findings provide valuable insights into the comprehensive assessment of reproductive health in dromedary camels.

Declaration of Competing Interest

None

Acknowledgements

We would like to thank H.H. Sheik Mohamed bin Rashid Al Maktum, UAE Prime minister and ruler of Dubai for his continuous moral and financial support of the project.

Appendix A. Supporting information

Supplementary data associated with this article can be found in the online version at [doi:10.1016/j.smallrumres.2024.107371](https://doi.org/10.1016/j.smallrumres.2024.107371).

References

- Agresti, A., 2018. Multiple regression and correlation. in: *Statistical Methods for the Social Sciences*. Pearson International, pp. 568–569.
- Al-Bulushi, S., Manjunatha, B.M., Bathgate, R., Rickard, J.P., de Graaf, S.P., 2018. Effect of semen collection frequency on the semen characteristics of dromedary camels. *Anim. Reprod. Sci.* 197, 145–153. <https://doi.org/10.1016/j.anireprosci.2018.08.022>.
- Al-Qarawi, A.A., 2005. Infertility in the dromedary bull: a review of causes, relations and implications. *Anim. Reprod. Sci.* 87, 73–92. <https://doi.org/10.1016/j.anireprosci.2004.11.003>.
- Ali, A., Derar, R., Al-Sobayil, F., Mehana, S., Al-Hawas, A., 2014. Impotentia generandi in male dromedary camels: clinical findings, semen characteristics, and testicular histopathology. *Theriogenology* 82, 890–896. <https://doi.org/10.1016/j.theriogenology.2014.07.001>.
- Almadaly, E., El-Kon, I., Heleil, B., Fattouh el, S., Mukoujima, K., Ueda, T., Hoshino, Y., Takasu, M., Murase, T., 2012. Methodological factors affecting the results of staining frozen-thawed fertile and subfertile Japanese Black bull spermatozoa for acrosomal status. *Anim. Reprod. Sci.* 136, 23–32. <https://doi.org/10.1016/j.anireprosci.2012.10.016>.
- Almadaly, E.A., Abdel-Salam, A.S., Sahwan, F.M., Kahilo, K.A., Abouzed, T.K., El-Domany, W.B., 2023. Fertility-associated biochemical components in seminal plasma and serum of buffalo (*Bubalus bubalis*) bulls. *Front Vet. Sci.* 9, 01–11. <https://doi.org/10.3389/fvets.2022.1043379>.
- Billah, M., Skidmore, J.A., 1992. The collection, evaluation and deep freezing of dromedary camel semen. 1st International Camel Conference. R and W publications, Dubai, UAE.
- Camela, E.S.C., Nociti, R.P., Santos, V.J.C., Macente, B.I., Maciel, G.S., Feliciano, M.A.R., Vicente, W.R.R., Gill, I., Bartlewski, P.M., Oliveira, M.E.F., 2017. Ultrasonographic characteristics of accessory sex glands and spectral Doppler indices of the internal iliac arteries in peri- and post-pubertal Dorper rams raised in a subtropical climate. *Anim. Reprod. Sci.* 184, 29–35.
- Camela, E.S.C., Nociti, R.P., Santos, V.J.C., Macente, B.I., Murawski, M., Vicente, W.R.R., Bartlewski, P.M., Oliveira, M.E.F., 2019. Changes in testicular size, echotexture, and arterial blood flow associated with the attainment of puberty in Dorper rams raised in a subtropical climate. *Reprod. Domest. Anim.* 54, 131–137. <https://doi.org/10.1111/rda.13213>.
- De Martino, C., Floridi, A., Marcante, M.L., Malorni, W., Scorza Barcellona, P., Bellocchi, M., Silvestrini, B., 1979. Morphological, histochemical and biochemical studies on germ cell mitochondria of normal rats. *Cell Tissue Res* 196, 1–22. <https://doi.org/10.1007/BF00236345>.
- Echegaray, A., Marcantonio, S., Maraboli, C., Muñoz, I., Escartín, N., Gnemmi, G., 2018. New echotexture parameters to evaluate the testicular parenchyma in bulls. 22th Annual Conference of the European Society for Domestic Animal Reproduction, Cordoba, Spain, *Reprod. Dom. Anim.*
- El-Bahrawy, K.A., Khalifa, M.A., Rateb, S.A., 2015. Recent advances in dromedary camel reproduction: An Egyptian field experience. *Emir. J. Food Agric.* 27, 350–354.
- England, G., Bright, L., Pritchard, B., Bowen, I.M., de Souza, M.B., Silva, L., Moxon, R., 2017. Canine reproductive ultrasound examination for predicting future sperm quality. *Reprod. Domest. Anim.* 52, 202–207. <https://doi.org/10.1111/rda.12825>.
- Escartín, N., Muñoz, I., Gil, A., Echegaray, A., 2018. New echotexture parameters to evaluate the testicular parenchyma in rams. 22th Annual Conference of the European Society for Domestic Animal Reproduction, Cordoba, Spain, *Reprod. Dom. Anim.*
- Eskandari, F., Momeni, H.R., 2016. Protective effect of silymarin on viability, motility and mitochondrial membrane potential of ram sperm treated with sodium arsenite. *Int. J. Reprod. Biomed.* 14, 397–402.
- Faye, B., Bonnet, P., 2012. Camel sciences and economy in the world: current situation and perspectives. 3rd ISOCARD Conference, Muscat, Oman, ISOCARD.
- Folgerø, T., Bertheussen, K., Lindal, S., Torbergsen, T., Oian, P., 1993. Mitochondrial disease and reduced sperm motility. *Hum. Reprod.* 8, 1863–1868. <https://doi.org/10.1093/oxfordjournals.humrep.a137950>.
- Garde López-Brea, J., 1992. Freezing semen in sheep: biological characteristics of thawed doses. PhD, Universidad Complutense de Madrid.
- Garner, D.L., Thomas, C.A., Allen, C.H., 1997. Effect of semen dilution on bovine sperm viability as determined by dual-DNA staining and flow cytometry. *J. Androl.* 18, 324–331.
- Giffin, J.L., Franks, S.E., Rodriguez-Sosa, J.R., Hahnel, A., Bartlewski, P.M., 2009. A study of morphological and haemodynamic determinants of testicular echotexture characteristics in the ram. *Exp. Biol. Med.* 234, 794–801. <https://doi.org/10.3181/0812-RM-364>.
- Guzick, D.S., Overstreet, J.W., Factor-Litvak, P., Brazil, C.K., Nakajima, S.T., Coutifaris, C., Carson, S.A., Cisneros, P., Steinkampf, M.P., Hill, J.A., Xu, D., Vogel, D.L., 2001. Sperm morphology, motility, and concentration in fertile and infertile men. *N. Engl. J. Med.* 345, 1388–1393. <https://doi.org/10.1056/NEJMoa003005>.
- Hafez, E.S., Hafez, B., 2001. Reproductive parameters of male dromedary and bactrian camels. *Arch. Androl.* 46, 85–98.
- Hess, R.A., Renato de Franca, L., 2008. Spermatogenesis and cycle of the seminiferous epithelium. *Adv. Exp. Med. Biol.* 636, 1–15 (<https://doi.org/>).
- Hsieh, M.L., Huang, S.T., Huang, H.C., Chen, Y., Hsu, Y.C., 2009. The reliability of ultrasonographic measurements for testicular volume assessment: comparison of three common formulas with true testicular volume. *Asian J. Androl.* 11, 261–265. <https://doi.org/10.1038/aja.2008.48>.
- Johnson, L., Welsh, T.H., Curley, K.O., Johnston, C.E., 2010. Anatomy and physiology of the male reproductive system and potential targets of toxicants. *Comprehensive Toxicology* (Second Ed). Elsevier, McQueen, C. A. Oxford, pp. 5–59. <https://doi.org/10.1111/ahc.12902>.
- Kasimanickam, V.R., Kasimanickam, R.K., Kastelic, J.P., Stevenson, J.S., 2013. Associations of adiponectin and fertility estimates in Holstein bulls. *Theriogenology* 79, 766–777. <https://doi.org/10.1016/j.theriogenology.2012.12.001>.
- Kastelic, J.P., Brito, L.F., 2012. Ultrasonography for monitoring reproductive function in the bull. *Reprod. Domest. Anim.* 47, 45–51. <https://doi.org/10.1111/j.1439-0531.2012.02042.x>.
- Kreit, E., Mätthger, L.M., Hanlon, R.T., Dennis, P.B., Naik, R.R., Forsythe, E., Heikenfeld, J., 2013. Biological versus electronic adaptive coloration: how can one inform the other? *J. R. Soc. Interface* 1–13. <https://doi.org/10.1098/rsif.2012.0601>.
- Kühn, A.L., Scortegagna, E., Nowitzki, K.M., Kim, Y.H., 2016. Ultrasonography of the scrotum in adults. *Ultrasonography* 35, 180–197. <https://doi.org/10.14366/ug.15075>.

- Lafuente, A., Lafuente, M., Escartin, N., Muñoz, I., Echegaray, A., 2018. New echotexture parameters to evaluate the testicular parenchyma in stallions. 22th Annual Conference of the European Society for Domestic Animal Reproduction, Cordoba, Spain.
- Laurent, M.R., Hammond, G.L., Blokland, M., Jardí, F., Antonio, L., Dubois, V., Khalil, R., Sterk, S.S., Gielen, E., Decallonne, B., Carmeliet, G., Kaufman, J.M., Fiers, T., Huhtaniemi, I.T., Vanderschueren, D., Claessens, F., 2016. Sex hormone-binding globulin regulation of androgen bioactivity in vivo: validation of the free hormone hypothesis. *Sci. Rep.* 1–12. <https://doi.org/10.1038/srep35539>.
- Malo, C., Crichton, E.G., Morrell, J.M., Pukazhenth, B.S., Skidmore, J.A., 2017. Single layer centrifugation of fresh dromedary camel semen improves sperm quality and in vitro fertilization capacity compared with simple sperm washing. *Reprod. Domest. Anim.* 52, 1097–1103. <https://doi.org/10.1111/rda.13036>.
- Malo, C., Echegaray, A., Juhasz, J., Nagy, P., Skidmore, J.A. (2018). New echotexture parameters to evaluate the testicular parenchyma in dromedary camel bulls. 2nd Conference of the International Society of Camelid Research and Development, Djerba, Tunisia.
- Malo, C., Grundin, J., Morrell, J.M., Skidmore, J.A., 2019. Individual male dependent improvement in post-thaw dromedary camel sperm quality after addition of catalase. *Anim. Reprod. Sci.* 209, 106–118. <https://doi.org/10.1016/j.anireprosci.2019.106168>.
- Marcantónio, S.A., 2020. Relationship between the echotexture of testicular parenchyma and seminal quality and sperm production in AI beef bull. Master, Universidad de Buenos Aires.
- Mitterberger, M., Horninger, W., Aigner, F., Pinggera, G.M., Steppan, I., Rehder, P., F. Frauscher, F., 2010. Ultrasound of the prostate. *Cancer Imaging* 10, 40–48.
- Moxon, R., Bright, L., Pritchard, B., Bowen, I.M., de Souza, M.B., da Silva, L.D., England, G.C., 2015. Digital image analysis of testicular and prostatic ultrasonographic echogenicity and heterogeneity in dogs and the relation to semen quality. *Anim. Reprod. Sci.* 160, 112–119. <https://doi.org/10.1016/j.anireprosci.2015.07.012>.
- Muñoz, I., Escartín, N., Zamora, A.E.A., 2018. New echotexture parameters to evaluate the testicular parenchyma in boars. 22th Annual Conference of the European Society for Domestic Animal Reproduction, Spain.
- Nicholas, F.W., 1996. Genetic improvement through reproductive technology. *Anim. Reprod. Sci.* 42, 205–214.
- Ntemka, A., Kioussis, E., Boscos, C., Theodoridis, A., Kourousekos, G., Tsakmakidis, I., 2018. Effects of testicular hemodynamic and echogenicity changes on ram semen characteristics. *Reprod. Domest. Anim.* 53, 50–55. <https://doi.org/10.1111/rda.13279>.
- Pasha, R.H., Lodhi, L.A., Jamil, H., 2010. Biometric and ultrasonographic evaluation of the testis of one-humped camel. *Pak. Vet. J.* 31, 129–133.
- Pelliccione, F., Micillo, A., Cordeschi, G., D'Angeli, A., Necozone, S., Gandini, L., Lenzi, A., Francavilla, F., Francavilla, S., 2011. Altered ultrastructure of mitochondrial membranes is strongly associated with unexplained asthenozoospermia. *Fertil. Steril.* 95, 641–646. <https://doi.org/10.1016/j.fertnstert.2010.07.1086>.
- Perumal, P., 2014. Scrotal circumference and its relationship with testicular growth, age, and body weight in Tho Tho (*Bos indicus*) bulls. *Int. Sch. Res. Not.*, 249537 <https://doi.org/10.1155/2014/249537>.
- Rated, S.A., 2006. Improving reproductive efficiency of sub-fertile one-humped bull camels under semi-arid conditions PhD, University of Alexandria.
- Skakkebaek, N.E., Rajpert-De Meyts, E., Buck Louis, G.M., Toppari, J., Andersson, M.L., Eisenberg, T.K., Jensen, N., Jørgensen, S.H., Swan, K.J., Sapra, S., Ziebe, A.M., Priskorn, L., Juul, A., 2016. Male reproductive disorders and fertility trends: Influences of environment and genetic susceptibility. *Physiol. Rev.* 96, 55–97. <https://doi.org/10.1152/physrev.00017.2015>.
- Skidmore, J.A., Malo, C.M., Crichton, E.G., Morrell, J.M., Pukazhenth, B.S., 2018. An update on semen collection, preservation and artificial insemination in the dromedary camel (*Camelus dromedarius*). *Anim. Reprod. Sci.* 194, 11–18. <https://doi.org/10.1016/j.anireprosci.2018.03.013>.
- Skidmore, J.A., Morton, K.M., Billah, M., 2013. Artificial insemination in dromedary camels. *Anim. Reprod. Sci.* 136, 178–186. <https://doi.org/10.1016/j.anireprosci.2012.10.008>.
- Swelum, A.A., Saadeldin, I.M., Ba-Awadh, H., Al-Mutary, M.G., Alowaimier, A.N., 2019. Effect of short artificial lighting and low temperature in housing rooms during non-rutting season on reproductive parameters of male dromedary camels. *Theriogenology* 131, 133–139. <https://doi.org/10.1016/j.theriogenology.2019.03.038>.
- Tan, K.A.L., De Gendt, K., Atanassova, N., Walker, M., Sharpe, R.M., Saunders, P.T.K., Denolet, E., Verhoeven, G., 2005. The role of androgens in Sertoli cell proliferation and functional maturation: Studies in mice with total or Sertoli cell-selective ablation of the androgen receptor. *Endocrinology* 146, 2674–2683. <https://doi.org/10.1210/en.2004-1630>.
- Thompson Jr., D.L., Pickett, B.W., Squires, E.L., Amann, R.P., 1979. Testicular measurements and reproductive characteristics in stallions. *J. Reprod. Fertil.* 27, 13–17.
- Trussell, J.C., Coward, R.M., Santoro, N., Stetter, C., Kunselman, A., Diamond, M.P., Hansen, K.R., Krawetz, S.A., Legro, R.S., Heisenleder, D., Smith, J., Steiner, A., Wild, R., Casson, P., Coutifaris, C., Alvero, R.R., Robinson, R.B., Christman, G., Patrizio, P., Zhang, H., Lindgren, M.C., 2019. Association between testosterone, semen parameters, and live birth in men with unexplained infertility in an intrauterine insemination population. *Fertil. Steril.* 111, 1129–1134. <https://doi.org/10.1016/j.fertnstert.2019.01.034>.
- Verze, P., Cai, T., Lorenzetti, S., 2016. The role of the prostate in male fertility, health and disease. *Nat. Rev. Urol.* 13, 379–386. <https://doi.org/10.1038/nrurol.2016.89>.
- Waheed, M.M., Ghoneim, I.M., Hassieb, M.M., Alsumait, A.A., 2014. Evaluation of the breeding soundness of male camels (*Camelus dromedarius*) via clinical examination, semen analysis, ultrasonography and testicular biopsy: a summary of 80 clinical cases. *Reprod. Domest. Anim.* 49, 790–796. <https://doi.org/10.1111/rda.12370>.
- Zhang, J.R., Zhang, P.Y., Sun, L.G., 2018. Mild androgen insensitivity syndrome: a case report. *Zhonghua Nei Ke Za Zhi* 57, 600–602. <https://doi.org/10.3760/cma.j.issn.0578-1426.2018.08.014>.